Multiscale analyses of pavement texture during polishing

Wiyao Edjeou, Véronique Cerezo, Hassan Zahouani, Ferdinando Salvatore

Multiscale analyses of pavement texture during polishing

Wiyao Edjeou[1], Veronique Cerezo[1], Hassan Zahouani[2], Ferdinando Salvatore[3]

[1] French Institute of Science and Technology in Transportation, Planning and Networks, Nantes
[2] Central School of Lyon
[3] National School of Engineers of Saint-Étienne.

wiyao.edjeou@ifsttar.fr

Abstract
Skid resistance is essential for road user safety and depends directly on the texture of the pavement. This texture is related to the surface texture of the aggregates. During its lifetime, the texture of the pavement evolves under the wear induced by road traffic. This phenomenon is called polishing. This paper presents a multiscale method based on the continuous wavelet decomposition of pavement texture to follow the evolution of the texture of aggregates during polishing at different scales. Several indicators are proposed to assess texture evolution and to correlate with friction evolution. The relevance of these parameters is assessed on samples composed of aggregates, which surface is characterized through laboratory experiments.
Keywords: surface texture, multiscale analysis, wavelet, polishing.

1. Introduction

The functional properties of pavements such as rolling noise, skid resistance and rolling resistance are closely related to the surface texture [1]. It is essential to be able to follow the evolution of this texture over time in order to predict pavement maintenance. Indeed, road skid resistance tends to decrease under traffic and climate actions. For a surface made of bituminous concrete, the skid resistance evolution involves a removal of the bitumen layer and a polishing of the aggregates [2, 3]. Moreover, texture is generally divided into two scales: microtexture and macrotexture. Microtexture is defined as surface irregularities whose dimensions range between 0.001 and 0.5mm vertically, and below 0.5mm horizontally (ISO 13473-1 2019) [4], whereas macrotexture covers a range between 0.1 and 20mm vertically, and between 0.5 and 50mm horizontally (ISO 13473-1 2019) [4]. This separation allows explaining the two main phenomena involved in friction generation (adhesion and hysteresis) but it is rather limited to really understand and explain the evolution of the road texture and more specifically the one of the aggregates that constitute it as well as road pavement skid resistance evolution.

Indeed, the texture of aggregates is composed of several scales of texture superimposed on each other. For a better understanding of friction evolution, it is essential to know the evolution of the texture of aggregates at each scale, which is not the case at this moment. Some attempts were done to connect standard texture parameters to skid resistance evolution but it remains rough [5–7]. More research is needed to tackle this issue.

Thus, existing texture acquisition methods developed in other fields like industry or aeronautics allow us to represent it as a signal on which operations like the Fourier transform [8, 9] can be applied. Usually, the texture signal is separated into different components using a filter [10]. The components that are obtained are the roughness, the undulation and the shape. After filtering, the texture parameters are calculated by averaging over the entire profile. Thus, it is impossible to access the information contained in the different scales of the profile as told previously.

Fast Fourier Transform (FFT) is a powerful tool for calculating the frequency components of texture signals. For periodic signals, it makes it possible to establish a relationship between the space domain and the frequency domain. Because the texture signals are random, the FFT can not be interpreted as multiscale decomposition.

To be able to separate the different scales, another method based on the Fourier transform, called the Short Time Fourier Transform (SFFT) can be used [11]. This method is based on the Gabor transform. But due to its fixed resolution in the spatial and frequency domains, it does not allow access to the real information contained in the texture signals.
The solution to our problem should imply to have a method with variable space-frequency resolution. The analysing window would be narrowed for high frequencies and extended for low frequencies. A method exhibiting these characteristics is the wavelet method [12, 13]. Until now, only discrete wavelet transform has been applied to study pavement macrotexture, which is a specific range of texture involved in friction forces generation [14, 15]. However, microtexture is a huge contributor to friction forces generation and continuous wavelet transform is a good candidate for signal series analysis due to its more fine scale discretization.
This paper proposes an approach based on continuous wavelet-based multiscale decomposition on aggregates before and after polishing. The objective is, on the one hand, to follow the evolution of each texture scale (from micro to macrotexture) during polishing. On the other hand, the objective is the definition of a relevant multiscale texture parameter which is able to traduce the texture evolution and which could be connected to skid resistance evolution during polishing. The paper is divided into four parts. The first part presents the nomenclature of parameters, which are used. The second part is a theoretical approach based on the wavelet method. It focuses on the choice of calculation parameters. The third part presents the experimentation led to develop and validate the method. It details the polishing and texture acquisition techniques used in the study. The last part presents the results and resulting interpretations.

2. Nomenclature

$x(t)$: Signal as a function of t
$\psi(t)$: Mother or basic wavelet function
$\psi(b,a)$: Daughter or analyzing wavelet
a $(\boldsymbol{\mu m})$: Contraction or scale parameter
b $(\boldsymbol{\mu m})$: Translation parameter
C_g : Energy of mother wavelet in Fourier space
$\widehat{\psi(\omega)}$: Fourier transform of mother wavelet
ψ_0 : Non-normalized wavelet
$W(a,b)$: Continuous wavelet transform of signal
ω_k : Angular frequency
FT : Fourier transform
FT^{-1} : Inverse Fourier transform
J : Number of scale
δj : Scale sampling parameter
δt $(\boldsymbol{\mu m})$: Signal sampling interval
N : Number of measured points
W_δ : Wavelet transform of δ function
C_δ : Constant corresponding to wavelet reconstruction of δ function
$\Re\{.\}$: Give the real value
Ra $(\boldsymbol{\mu m})$: Arithmetic mean
$RMS(rms)(\boldsymbol{\mu m})$: Root mean square

3. Wavelet method

The wavelet method is a flexible time-frequency method. The analysing functions for each resolution are obtained by translation and contraction of a basic function. If $\psi(t)$ is the basic wavelet function, the analysing functions are obtained by equation (1):

$$\psi(b,a) = \frac{1}{\sqrt{a}}\psi\left(\frac{t-b}{a}\right) \quad (1)$$

where a represents the contraction coefficient, characterizing the analysis scale and b the translation coefficient.

The wavelet function must be of finite energy and square-integral for each of its variables, $\psi(b,a)\varepsilon L^2(\Re)$.

Then the following admissibility condition must be checked:

$$C_g = \int_{-\infty}^{+\infty} |\widehat{\psi(\omega)}|^2 \frac{d\omega}{|\omega|} < \infty \quad (2)$$

With $\widehat{\psi(\omega)}$ the Fourier transform of $\psi(t)$. This amounts to saying that the average of $\psi(t)$ is zero:

$$\psi(\omega = 0) = \int_{-\infty}^{+\infty} \psi(t)dt = 0 \quad (3)$$

The wavelet transform of a function $x(t)$ is:

$$W(a,b) = \frac{1}{\sqrt{a}} \int_{-\infty}^{+\infty} x(t)\psi^*(\frac{t-b}{a})\, dt \quad (4)$$

The wavelet coefficient $W\,(a,b)$ is a function of the variable t, but also of a and b. ψ^* represents the conjugate of ψ.

If the eligibility conditions are met, the inverse transform is defined by equation (5):

$$x(t) = \frac{1}{C_g} \int_{-\infty}^{+\infty} \int_{-\infty}^{+\infty} \frac{1}{\sqrt{a}} W_{a,b}(t)\psi(\frac{t-b}{a}) \frac{dadb}{a^2} \quad (5)$$

The wavelets must be normalized to be able to compare wavelet transforms at different scales. To reduce the calculation time, the calculations are made in the frequency domain. The normalized wavelet in the Fourier space is given by equation (6):

$$\hat{\psi}(a\omega_k) = \sqrt{(\frac{2\pi a}{\delta t})}\hat{\psi}_0\big((a\omega_k)\big) \quad (6)$$

where $\hat{\psi}$ is the Fourier transform of ψ, a the scale, ω_k is the angular frequency in the frequency domain, δt is the sampling period and k is the frequency index. ψ_0 is the non-normalized wavelet.

Equation (7) gives the formula for calculating the angular frequency:

$$\omega_k = \begin{cases} \frac{2\pi k}{N\delta t} : k \leq N/2 \\ -\frac{2\pi k}{N\delta t} : k > N/2 \end{cases} \quad (7)$$

where N is the number of measured points.

The wavelet transform of a signal $x\,(t)$ is the inverse Fourier transform of the product of the Fourier transforms of $x\,(t)$ and the wavelet:

$$W_n(a) = FT^{-1}(\sum_{k=0}^{n} \hat{x}_k \hat{\psi}^*(a\omega_k) e^{i\omega_k n\delta t}) \quad (8)$$

where n corresponds to the position.

The scales of the wavelet transform are obtained by equation (9):

$$a_j = a_0 2^{j\delta j}, j = 1,..,J \quad (9)$$

a_0 is the smallest scale and is equal to $a_0 = 2\delta t$.

δj corresponds to a parameter allowing to sample the scales.

For the Morlet wavelet, the maximum value of this parameter ensuring a good sampling corresponds to 0.5 [16]. For the other wavelets, a value greater than 0.5 does not influence the sampling. On his side, Torrence [16] obtained a good sampling by using a value of 0.25. This value is considered in our study.

In equation (9), j is the scale number and J is the scale number. The number of scales ensuring a good decomposition of the texture is given by equation (10):

$$J = \delta j^{-1} log_2(\frac{N\delta t}{a_0}) \quad (10)$$

Since the wavelet transform is a band pass filter, it is possible to reconstruct the start signal. This transform introduces redundancy into space and frequency. Thus, one can use a wavelet different from that used for decomposition for reconstruction. A simple way to do this reconstruction is to use delta function δ [17].

The reconstruction of the signal $x\ (t)$ for each scale is expressed by equation (11):

$$x_{j,n} = \frac{\delta j \delta t^{1/2}}{C_\delta \psi_0(0)} \frac{\Re\{W_{j,n}(a_j)\}}{{a_j}^{1/2}} \quad (11)$$

$\psi_0(0)$ is used to suppress the energy of the scale. C_δ is a constant coming from the reconstruction of the function δ. The wavelet transform of the δ function is:

$$W_\delta(a) = \left(\frac{1}{N}\right) \sum_{k=0}^{N-1} \hat{\psi}^*(a\omega_k) \quad (12)$$

C_δ is then obtained by the formula in equation (13):

$$C_\delta = \frac{\delta j \delta^t 1/2}{\psi_0(0)} \sum_{j=0}^{J} \frac{\Re\{W_\delta(a_j)\}}{{a_j}^{1/2}} \quad (13)$$

$\Re\{W_{n,j}(a_j)\}$ corresponds to the real part of $W_{n,j}(a_j)$. If $x\ (t)$ is a complex function, the imaginary part of $W_{n,j}(a_j)$ will also be considered in the reconstruction.

The signal $x\ (t)$ is obtained by summing for each position the values of $x\ (t)$ at each scale :

$$x_i = \sum_{j=1}^{J} x_{j,i} \quad (14)$$

4. Experimental study

The experimental study has two objectives. The first one is to reproduce in the laboratory the effect of polishing on various aggregates types. The second one is to map the surfaces before and after polishing and to output a texture signal well adapted to multiscale analysis of its evolution.

4.1 Samples

Samples are circular discs $225\ mm$ in diameter. This disc is made by molding. The method and the materials of manufacture are similar to those used in [5]. The aggregates (fraction $7.2\ /\ 10\ mm$) are placed in the mold on their flat face on one layer. These aggregates are placed as close as possible to each other. The spaces between the aggregates are filled with silica and Fontainebleau sand (fraction $0.16\ /\ 0.315\ mm$). The mold is then filled in with resin. The choice of resin result from the fact that it represents a good compromise between maneuverability (to ensure that all voids are fill in by the resin), convenience (lower toxicity) and setting time. Once all is solidified, we remove the sample (see figure 1). The mosaic is prepared with aggregates extracted from a quarry in New Zealand. Aggregates used is Greywacke. It consists of fine grain minerals that are supported by a matrix that is rich in very angular shaped Quartz.

Figure 1: Example of a sample made of pure aggregates

4.2 Polishing tests

The aim of the polishing test is to reproduce the evolution of the road texture due to the traffic. A commonly used polishing method has been developed by the Transport and Road Research Laboratory (TRRL). This test is known as Polished Stone Value (PSV) [18]. But this polishing technique is very rough and not suitable for evaluating the evolution of the properties of aggregates from road surfaces [19]. The polishing performed by the Wehner and Schulze machine makes it possible to reproduce polishing due to road traffic [14]. The machine is composed of a polishing station simulating the action of traffic and an adhesion measuring station simulating the braking of a wheel in the presence of water. Figure 2 shows the different parts of the machine.

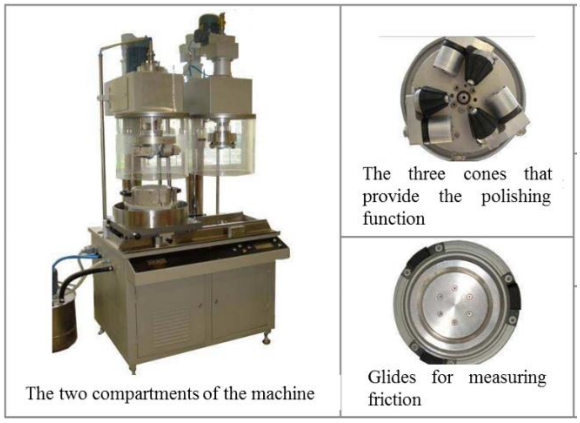

Figure 2: Wehner and Schulze

Polishing is done by rolling with a slight slip of three rubber cones on the sample. The polishing station is fed continuously with a mixture of water and silica flour which constitutes the abrasive. The polishing is carried out at $500\,rpm$, ie $17\,km/h$. The contact pressure between the polishing cones and the sample is $0.4\,N/mm^2$. The tests carried out by the Wehner and Schulze machine are standardized (NF EN 12697-49) [20]. The measurements led to a curve giving the evolution of friction coefficient with polishing stages.

4.3 Texture acquisition

The goal is to map the surface of the sample before and at different stages of polishing. In the sample, two randomly areas of dimensions $5\,mm * 5\,mm$ are studied (Figure 3). This random choice is ensured by the fact that aggregates are relatively homogeneous in terms of aspect (Figure 1). The number of selected areas can seem to be low. But, as the measuring of texture is time-consuming, a compromise had to be found.

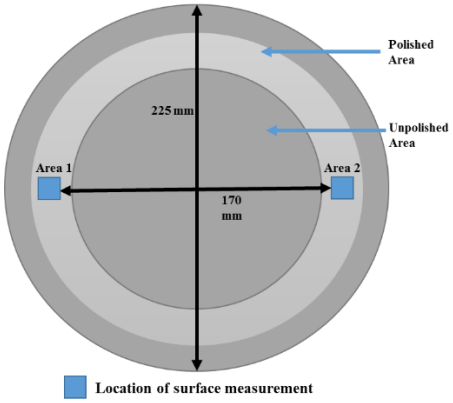

Figure 3: Sample with mapping zones

Each area is identified by marking with paint. This guarantees the mapping of the same area before and after polishing.

The acquisition of the maps is done with the Alicona Infinite Focus sensor. This sensor allows us to make a three-dimensional optical measurement of the roughness of the surface. The measurement principle is based on the focal variation.

A sample is placed on a moving table and illuminated by modulated lighting. The optical sensor incorporates a digital sensor inside that captures the light reflected by the sample. During the movement of the table on which the sample is placed, the position of each point of the sample is determined by the variation of the contrast.

Figure 4 shows the apparatus and result which is obtained.

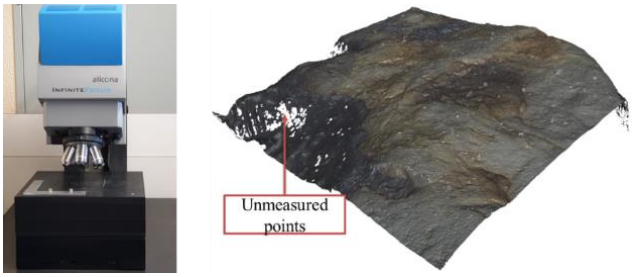

Figure 4: Alicona

This unit allows us to map for the following magnifications: $2.5\ \times, 5\ \times, 10\ \times, 20\ \times, 50\ \times$ and $100\ \times$.

A compromise had to be found between the time of measurement and precision. Then, the measurements were made at $20\ \times$ magnification. Indeed, the vertical and lateral resolutions at this magnification are respectively $59\ nm$ and $438\ nm$. These are sufficient for the present study if we take into account the dimensions of the irregularities constituting the texture.

After this mapping, the data are exported in the MountainsMap version 7 software. This software allows us to perform several operations such as the filling of the unmeasured points, the straightening of the surface, the removal of the shape, the extraction of the profiles, 2D visualization of the surface.

The maximum slope measurable by the sensor is $87°$. MountainsMap has been used to remove slopes exceeding $87°$ which constitute outliers.

The unmeasured points are covered with a "soft form". This shape fits best with the outline. It is a kind of mathematical scarring.

To carry out the detailed characterization of a surface, one must previously apply a pretreatment to eliminate its shape and its slope. This slope was obtained by fitting the original surface with the first-order mean square plane. Surface shape has also been removed by determining the seventh-order mean square plane.

Figure 5 shows different results that have been obtained after different operations.

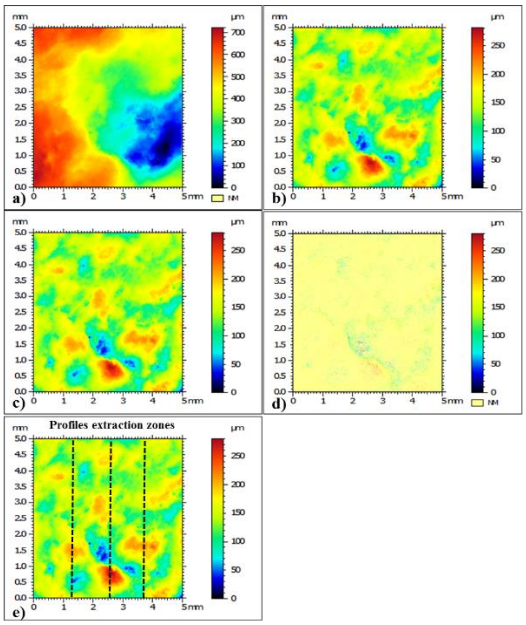

Figure 5: a) Original surface, b) Surface after shape suppression, c) Surface after slope suppression, d) Outliers determined by MountainsMap, e) surface after outliers suppression with profiles extraction zones

In each area, three profiles are extracted. Then, we have six profiles for the two zones for different degrees of polishing. If we consider all the polishing degrees, then we have thirty profiles. This number of profiles can be considered as important if we take into account the acquisition time and precision of measurements.

4.4 Experimental protocol

This part summarizes the experimental protocol. The following steps are followed :

- After making the disc, a texture measurement in the initial state is made.
- Afterward, the disc is polished up to 20 000 rotations. After that, a texture measurement is made. Before each texture measurement, the disc is washed.
- Polishing is continued until 50 000 rotations followed by a texture measurement.
- After this texture measurement, the polishing is continued until 90 000 rotations. This is also followed by a texture measurement.
- Finally, polishing is continued until 180 000 rotations. A final texture measurement is done.

5. Results and interpretations

This section presents the analysis of the extracted profiles, the choice of the analyzing wavelet and the application of the wavelet method to assess polishing.

4.1 Analyses of extracted profiles and their heights distribution

Figure 6 exhibits an example of five profiles extracted at different polishing stages in both zones at the same position.

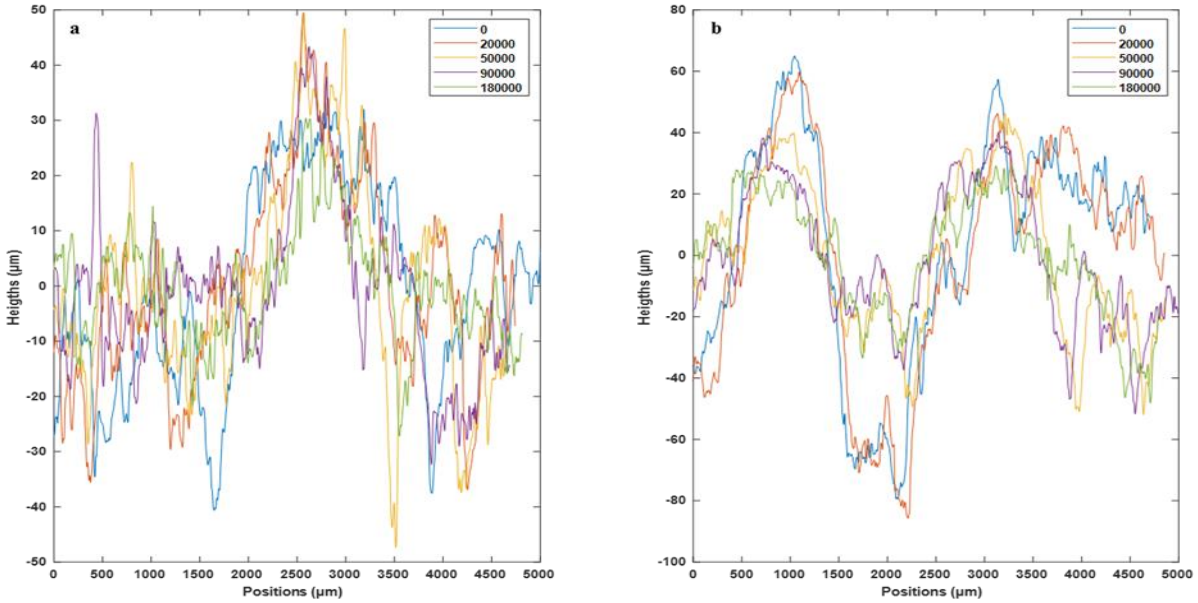

Figure 6: Extracted profiles in : a) Area 1, b) Area 2

On figure 6, 0 (initial state), 20 000, 50 000, 90 000 and 180 000 denoted the degree of polishing. These figures do not allow *a priori* to detect the effect of polishing. Thus, the distributions of heights have also been traced (Figure 7).

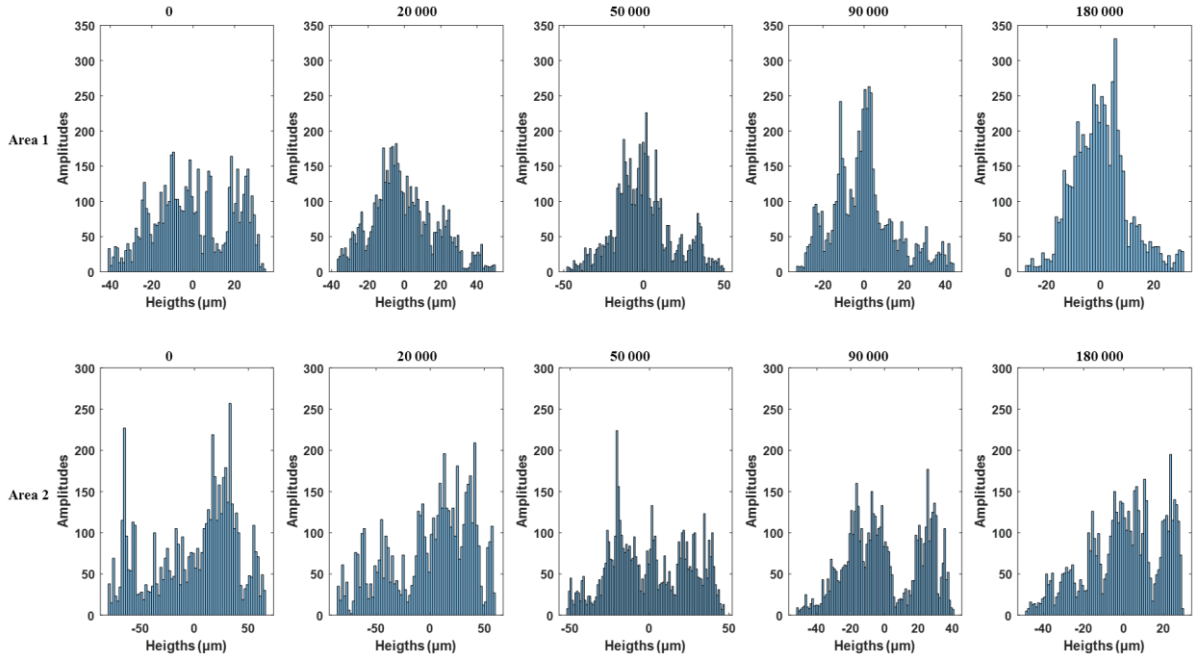

Figure 7: Heights distribution at various polishing stages

In Figure 7, we notice a decrease in the height of large asperities during the polishing process. This can be explained by the fact that during polishing, the cones of the Wehner and Schulze machine come into first contact with the large asperities.

We also notice an increase in small heights with polishing. This can be explained by the recirculation flow [21]. During polishing, there are two phenomena in competition: particle detachment and particle ejection. As the detachment flow is higher than ejection flow, some of the aggregates torn off by polishing fill the gaps between the asperities and are compacted. Thus, it seems that there is a disappearance and recreation of the texture during polishing.

4.2 Analysing wavelet choice

After analyses of extracted profiles, we focus on the application of the wavelet method. The first step concerns the determination of the most suitable wavelet to analyze the texture of road pavement aggregates. In the literature, Mezghani et al [22] recommends using either the Morlet wavelet or the eighth Gaussian derivative.

The Morlet wavelet [16] is given by equation (15):

$$\psi_0(t) = \pi^{-1/4} e^{i\omega_0 t} e^{-t^2/2} \tag{15}$$

With t the position parameter of the wavelet. The adimensional frequency $\omega_0$was chosen equal to 6 [16] to satisfy the conditions of admissibility of a wavelet.

Eighth Gauss wavelet [16] is given by equation (16):

$$\psi_0(t) = \frac{(-1)^{m+1}}{\sqrt{\Gamma\left(m+\frac{1}{2}\right)}} \frac{d^m}{dt^m}\left(e^{-\frac{t^2}{2}}\right) \tag{16}$$

With m the order of the derivative.

Figure 8 shows the results of the decomposition of an aggregate texture profile by using the two wavelets.

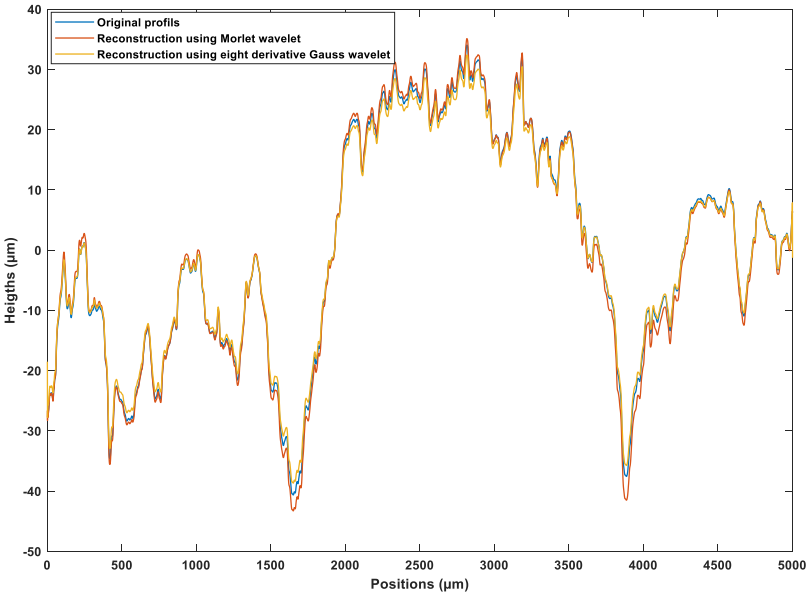

Figure 8: Reconstruction of the original profile using the Morlet wavelet and the Gauss wavelet

Visually, we can not distinguish the wavelet giving the most faithful reconstruction.

In pavement surface analyses, the average height is often used to assess the texture. We use this parameter to verify the accuracy of reconstruction. The calculation formula is given by the following equation (17):

$$Ra = \left(\frac{1}{N}\right) \sum_{i=1}^{N} |x_i| \tag{17}$$

N is the number of measured points, x_i the value of the profile at point i. $|x_i|$ represents the absolute value of x_i. Table 1 shows the comparison of average heights between the three profiles.

Table 1: Reconstruction errors

Profiles	Original profile	Reconstruction using Morlet wavelet	Reconstruction using eighth Gauss wavelet
$\boldsymbol{Ra}$ $(\boldsymbol{\mu m})$	15.8	16.2	14.9
Relative error $\boldsymbol{\varepsilon}$ (%)	0	3	6

Table 1 shows that Morlet wavelet provides the best reconstruction. The same calculations have been done for all profiles (thirty profiles). By using Morlet wavelet, we have an average reconstruction error of 4% with a standard deviation of 1.4. By using eighth derivative of Gauss wavelet, we have an average reconstruction error of 5 % with a standard deviation of 0.01. Similar observations have been done with magnifications $5\ \times$ and $10\ \times$.

Increasing the degree of the Gaussian derivative would allow for a more faithful reconstruction. But, due to the computation time due to the numerical derivatives, we decided to implement the Morlet wavelet.

4.3 Application of wavelet multiscale decomposition

[2] found that skid resistance is related to root mean square (rms). On dry surface, skid resistance slightly decreases with rms. Indeed, on dry surface, skid resistance is related to contact area, which decreases with increasing rms. Conversely, on wet surface, skid resistance sharply increases with rms. On wet surface, high rms increases contact area. Figure 9 shows the evolution of rms during surface polishing.

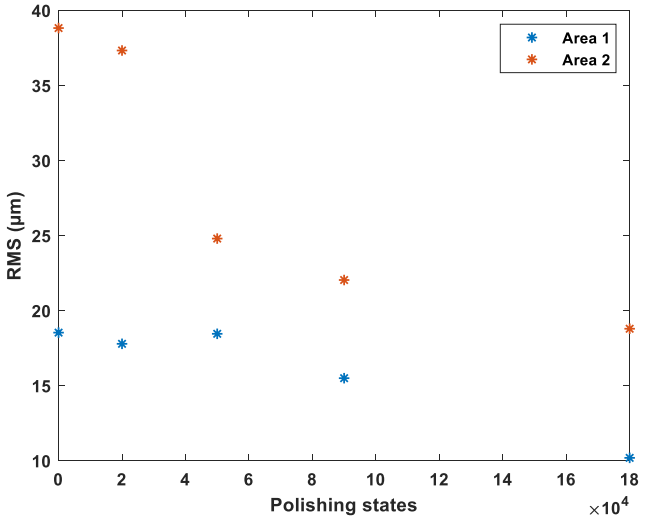

Figure 9 : RMS evolution

We can note a reduction of rms with polishing. Depending on wetting state of area (dry or wet), we will have increasing or decreasing of skid resistance. However, figure 9 do not allow to know how each scale evolve. To tackle this problem, the continuous wavelet transform is performed for the different profiles. In order to quantify the weight of each scale, rms has been calculated on each profile obtained at each scale. This parameter can be interpreted as the square root of normalized energy [14] at different scale. A graphic representation of obtained result is shown on figure 10.

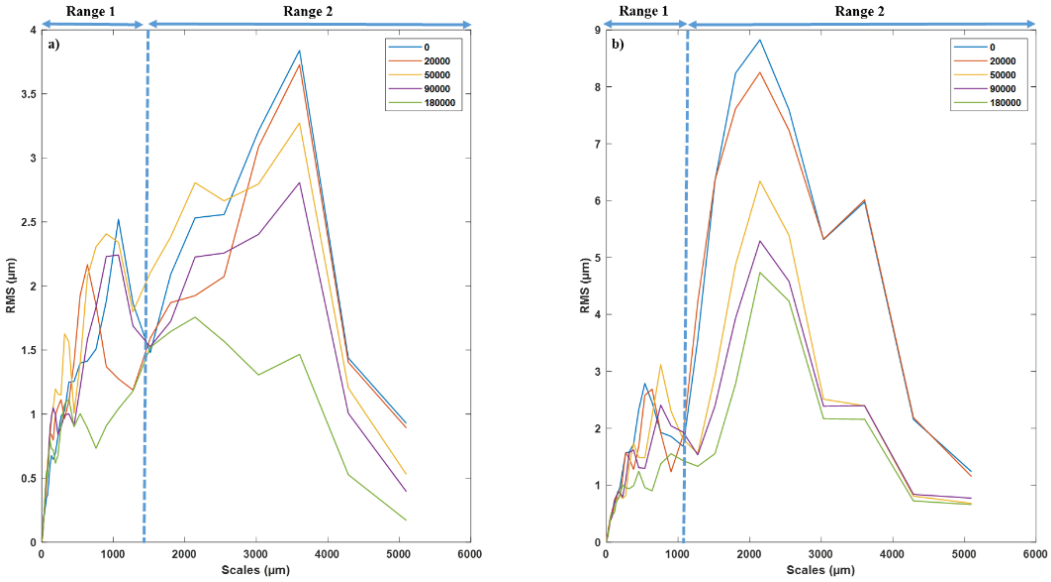

Figure 10 : Multiscale parameter evolution

On figure 10, we have overall a decrease of rms with polishing. However, depending on scale range, we do not have the same diminution rate.

On Area 1, for scale range, $0 - 1400\ \mu m$, there not great difference between each polishing state. Then we can say that, that range will not have great influence on skid resistance evolution. Beyond this range, we note clearly the decreasing of rms with polishing. Therefore, this scale will have great influence on skid resistance evolution. Similar observations can be made on Area 2. These observations show the importance of this multiscale analysis. It will help for accurate friction law definition.

6. Conclusions

In conclusion, we can say that the continuous wavelet transform can be used for multiscale decomposition of the texture of aggregates used in pavement composition. For the continuous wavelet transform, the wavelet providing, with a small computation time, a good decomposition is the Morlet wavelet. This study has been done on thirty profiles due to data acquisition time.

For the quantification of the weight of each texture scale, the spectrum of the amplitudes of rms of each scale can be used. This spectrum allows us to follow the evolution of the amplitude of each scale during polishing. This parameter will be used to define the effect of each scale of texture on skid resistance.

This method will be extended to pavement surface analysis like bituminous concrete. An in-depth study will be done on the creation of texture due to polishing.

Acknowledgments

This work is part of the I-Street project funded by Ademe and led by Eiffage. Thanks are due to Flavien Geisler, pilot of the I-Street project and Simon Pouget, coordinator of the module "Enrobé du Futur". The authors would like to thank Christophe Ropert for the fabrication of the specimens and the realization of the experiments.

Références

1. Do, M.-T.: Contribution des échelles de texture routière à l'adhérence des chaussées. (2004)
2. Do, M.-T., Cerezo, V.: Road surface texture and skid resistance. Surface Topography: Metrology and Properties. 3, 043001 (2015). https://doi.org/10.1088/2051-672x/3/4/043001
3. Do, M.-T., Tang, Z., Kane, M., Larrard, F. de: Pavement polishing—Development of a dedicated laboratory test and its correlation with road results. Wear. 263, 36–42 (2007). https://doi.org/10.1016/j.wear.2006.12.086

4. ISO 13473-1: Characterization of pavement texture by use of surface profiles – Part 1: determination of mean profile depth. ISO Standard, (2019)
5. Nataadmadja, A.D., Do, M.T., Wilson, D.J., Costello, S.B.: Quantifying aggregate microtexture with respect to wear—Case of New Zealand aggregates. Wear. 332–333, 907–917 (2015). https://doi.org/10.1016/j.wear.2014.11.028
6. Zahouani, H., Vargiolu, R., Do, M.T.: Characterization of microtexture related to wet road/tire friction. Proceedings of the 4th international symposium on pavement surface characteristics. 195–205 (2000)
7. Cerezo, V., Ropert, C., Hichri, Y., Do, M.-T.: Evolution of the road bitumen/aggregate interface under traffic-induced polishing. Proceedings of the Institution of Mechanical Engineers, Part J: Journal of Engineering Tribology. 233, 1433–1445 (2019). https://doi.org/10.1177/1350650119829370
8. Himeno, K., Nakamura, Y., Kawamura, A., Saito, K.: Skid resistance of asphalt pavement surfaces related to their microtexture. Procedings of International Symposium on Pavement Surface Characteristics. 207–216 (2000)
9. Samuels, S.E.: The feasibility of measuring road surface microtexture by means of laser techniques. (1986)
10. ISO NF EN 16610-21: Spécification géométrique des produits (GPS) : Filtrage. (2012)
11. Martin, V., JELENA, K.: Wavelets and subband coding. , New Jersey (1995)
12. Chen, X., Raja, J., Simanapalli, S.: Multi-scale analysis of engineering surfaces. International Journal of Machine Tools and Manufacture. 35, 231–238 (1995). https://doi.org/10.1016/0890-6955(94)P2377-R
13. Wolf, D., Husson, R.: Application des ondelettes à l'analyse de texture et à l'inspection de surface industrielle. Journal de Physique III. 3, 2133–2148 (1993). https://doi.org/10.1051/jp3:1993266
14. Zelelew, H., Khasawneh, M., Abbas, A.: Wavelet-based characterisation of asphalt pavement surface macro-texture. Road Materials and Pavement Design. 15, 622–641 (2014). https://doi.org/10.1080/14680629.2014.908137
15. Zelelew, H.M., Papagiannakis, A.T., Izeppi, E.D. de L.: Pavement macro-texture analysis using wavelets. International Journal of Pavement Engineering. 14, 725–735 (2013). https://doi.org/10.1080/10298436.2012.705004
16. Torrence, C., Compo, G.P.: A Practical Guide to Wavelet Analysis. Bulletin of the American Meteorological Society. 79, 61–78 (1998). https://doi.org/10.1175/1520-0477(1998)079<0061:APGTWA>2.0.CO;2
17. Farge, M., Schneider, K.: Wavelet transforms and their applications to MHD and plasma turbulence: a review. Journal of Plasma Physics. 81, 435810602 (2015). https://doi.org/10.1017/S0022377815001075
18. ISO NF EN 1097-8: Essais sur les propriétés mécaniques et physiques des granulats. Partie 8 : Détermination du coefficient de polissage accéléré. (2000)
19. Dunford, A.: The wehner schulze machine and its potential use to improve aggregate specification
20. French standard: Bituminous mixtures - test methods for hot mix asphalt - Part 49: Determination of friction after polishing. (2013)
21. Fillot, N., Iordanoff, I., Berthier, Y.: Wear modeling and the third body concept. Wear. 262, 949–957 (2007). https://doi.org/10.1016/j.wear.2006.10.011
22. Mezghani, S., Sabri, L., Mansori, M.E., Zahouani, H.: On the optimal choice of wavelet function for multiscale honed surface characterization. Journal of Physics: Conference Series. 311, 012025 (2011). https://doi.org/10.1088/1742-6596/311/1/012025